FISEVIER

Contents lists available at ScienceDirect

Remote Sensing of Environment

journal homepage: www.elsevier.com/locate/rse



Spring and summer monthly MODIS LST is inherently biased compared to air temperature in snow covered sub-Arctic mountains



Scott N. Williamson ^{a,*}, David S. Hik ^a, John A. Gamon ^{a,b}, Alexander H. Jarosch ^c, Faron S. Anslow ^d, Garry K.C. Clarke ^e, T. Scott Rupp ^f

- ^a Department of Biological Sciences, University of Alberta, Edmonton, Alberta T6G 2E9, Canada
- ^b Department of Earth and Atmospheric Sciences, University of Alberta, Edmonton, Alberta T6G 2E3, Canada
- ^c Institute of Earth Sciences, University of Iceland, Sturlugata 7, 101 Reykjavik, Iceland
- ^d Pacific Climate Impacts Consortium, University of Victoria, Victoria, British Columbia V8W 3R4, Canada
- e Department of Earth, Ocean and Atmospheric Sciences, University of British Columbia, Vancouver, British Columbia, V6T 1Z4, Canada
- f Scenarios Network for Alaska & Arctic Planning, University of Alaska, Fairbanks, AK 99709, USA

ARTICLE INFO

Article history: Received 10 June 2016 Received in revised form 29 October 2016 Accepted 14 November 2016 Available online 23 November 2016

Keywords: MODIS LST Downscaled NARR SNAP Snow cover Cloud cover Cryosphere

ABSTRACT

Satellite-derived land surface temperature (skin temperature) provides invaluable information for data-sparse high elevation and Arctic regions. However, the relationship between satellite-derived clear-sky skin temperature and various downscaled air temperature products for snow covered sub-Arctic alpine regions remain poorly understood, such that trend analysis or air temperature product integration is difficult. We compared monthly average air temperatures from two independent downscaled temperature products to MODIS Land Surface Temperature (LST) and air temperature at nine meteorological stations situated above tree-line in the southwest Yukon, Canada, between May and August 2008 for a full range of snow cover fractions. We found that both downscaled products generally agreed with LST for the low elevation, snow-free, vegetation classes. However, a systematic cold bias in Average LST emerged for snow fractions greater than approximately 40%, and this bias increased in magnitude as snow cover increased. In these situations the downscaled air temperatures were 5-7 °C warmer than Average LST for snow fractions of >90%, and this pattern was largely independent of the number of measurements of LST within a month. Maximum LST was similar to average air temperatures for high snow fractions, but Minimum LST was colder by 10 °C or more for all snow fractions, Consequently, the average of Maximum and Minimum LST produces the cold bias, compared to air temperature, for high snow cover fractions. Air temperature measured at nine meteorological monitoring stations located between elevations of 1408–2690 m, on land cover classes Barren, Sparsely Vegetated or Permanent Snow and Ice, confirmed the cold bias results when incorporating Minimum LST in monthly averages. For snow fractions of <40% the RMSE for all of the temperature products was < 2.5 $^{\circ}$ C when compared to station air temperature and all biases were positive and <2.0 °C. For snow fractions of >40%, the average LST bias became strongly negative at -4.5 °C, and the RMSE increased to 6.1 °C, whereas the downscaled products bias and RMSE were similar to those from snow fractions of < 40%. A weak warm bias for all the temperature products occurred for small snow fractions over non-forested land cover classes. Downscaled air temperature fields show physically real differences from Average LST in spring and summer, caused by snow cover and the interplay of Maximum and Minimum LST. These findings indicate that the integration of MODIS LST with downscaled air temperature products or local air temperature requires the incorporation of snow cover.

© 2016 Elsevier Inc. All rights reserved.

1. Introduction

Northern Hemisphere high latitudes, particularly Yukon and Alaska, have warmed an average of 1–3 °C over the last 50 years (Arctic Climate Impact Assessment – ACIA, 2005; Snow, Water Ice, Permafrost in the Arctic - SWIPA, 2011), and the Arctic in general has warmed by approximately 2 °C since 1950 (AMAP, 2012). This warming is coincident with

* Corresponding author. E-mail address: snw@ualberta.ca (S.N. Williamson). North American snow cover reduction, which contributes to the amplification of high latitude warming (Serreze et al., 2009). In addition to amplified warming at high latitudes compared to lower latitudes, high elevations are experiencing amplified warming compared to lower elevations (Pepin et al., 2015). Both high latitudes and high elevations suffer from information gaps because these regions are difficult to access, often have extreme weather which hampers monitoring, and are snow-covered most of the year. Existing instrumental air temperature measurements at high latitudes and elevation are sparse, sporadic and are often from heterogeneously placed monitoring locations, typically

at valley bottoms in mountainous terrain or coastal areas in the Arctic (Vincent and Mekis, 2006; Robeson, 1995). Two techniques are increasingly employed to generate continuous temperature products of sufficient spatial resolution to address questions about climate processes that occur at the landscape scale in the Arctic and at high elevation: thermal infrared remote sensing and climate downscaling.

The length of the satellite observation record of skin temperature (e.g., Comiso, 2003) is much shorter than instrumental records, and began in the early 1980s, but is an increasingly common method for trend analysis due to the progressively longer period over which these measurements have been acquired. The launch of the MODerate resolution Imaging Spectroradiometer (MODIS) in early 2000s marked a change toward an increase in data quality and quantity of thermal data that improves the measurement of skin temperature over previous methods. This is especially true as Earth observing satellites have proliferated since the introduction of MODIS. The new sensors and satellite platforms are better equipped to provide an improved treatment of many longstanding problems, such as orbital drift, cloud contamination, emissivity assessment and poor spatial resolution that made (and still make) the interpretation of skin temperature derived from satellite measurement difficult, especially in relation to air temperature (Jin and Dickinson, 2010). The relationship between long term clear-sky skin temperature and air temperature trends are often different because of the influence of cloud cover (Westermann et al., 2012; Østby et al., 2014). Furthermore, the influence of Canadian high Arctic land cover and season influences the accuracy and sensitivity of LST to land cover change (Muster et al., 2015).

Thermal infrared satellite observations are 'clear sky' which provides a version of skin temperature that is skewed to a specific set of atmospheric and surface illumination conditions. Infrared satellite observations of the Earth are dependent on the time of capture, and require conversion to more generalised metrics such as daily averages to increase their utility. Jin and Dickinson (1999) indicated that maximum daily infrared temperature, under clear sky conditions will correspond to peak solar insolation with an adjustment for phase lag. Thus maximum skin temperature occurs when the post-solar noon incoming radiation is balanced by outgoing radiative loss, or zero net radiation, and might occur up to several hours after solar noon. Satellite derived skin temperature values acquired several hours after solar noon will provide the highest correlations to air temperature because of the radiative surface heating and upward heat fluxes (Oke, 1987); minimum surface air temperature will occur at or slightly before sunrise (Sellers, 1965). Westermann et al. (2012) found that on Svalbard the incorporation of wintertime minimum infrared Land Surface Temperature (LST) into long-term averages caused a cold bias compared to in-situ measurements of skin temperature. This phenomenon is explained by cloud cover increasing the average minimum skin temperature, compared to the clear sky satellite observations of MODIS Land Surface Temperature.

Much recent work has focused on defining the relationship between air temperature and skin temperature although they are in fact separate physical entities that respond to the same forcing over different time scales (Jin and Dickinson, 2010). Strong correlations between LST and air temperatures for many vegetated land cover types typically produce an error (Root Mean Square Deviation) of approximately 2–3 °C (Zaksek and Schroedter-Homscheidt, 2009) irrespective of the methodology and of the spatial or temporal resolutions. Some comparisons between satellite remote sensing of skin temperature and downscaled air temperature measurements (e.g., NARR - the North American Regional Re-analysis product) are available (Royer and Poirier, 2010), indicating a 1 °C warm bias in the downscaled measurements compared to microwave skin temperature for snow-free conditions. Both the microwave skin temperatures and NARR were compared at a coarse spatial resolution of 25 and 32 km grid cells respectively. André et al. (2015) combined MODIS LST with horizontal and vertical polarizations from 37 GHz SSM/I-SSMIS for Arctic to produce a 25 km grid cell sizing skin temperature product. The combined product compares favourably (RMSE 2.2 K) to MODIS LST and has the added benefit of being able to image the ground through cloud, although at a relatively coarse spatial resolution. Permafrost mapping has also been conducted for the North Atlantic permafrost region through the combination of MODIS LST and re-analysis data using a 1 km grid cell (Westermann et al., 2015).

Downscaling of near-surface air temperatures can be produced at much higher spatial resolution than LST measurement (thermal infrared or microwave) and are not reliant on emissivity correction or clear sky observations. The downscaling method is typically either statistical or dynamical and can be applied to interpolated meteorological air temperature measurements or atmospheric temperature profiles. Further information regarding downscaling methodology is provided below in the methods section.

Optical remote sensing provides a good method for the detection of snow cover extent at high spatial resolution, but only in clear sky conditions. MODIS provides a measure of snow cover using an algorithm based on the normalised difference snow index (NDSI), normalised difference vegetation index for forested areas, a thermal mask and cloud mask (Hall et al., 2002). The snow cover product used in this study is the MODIS Terra daily fractional snow cover product produced at 500 m resolution (MOD10A1) determined through regression equations of NDSI and fractional snow cover (e.g., Salomonson and Appel, 2004). The MODIS sensor on the AQUA platform uses band 7 in the NDSI algorithm instead of band 6 as used on MODIS Terra. This causes poorer accuracy for AQUA snow products (Hall and Riggs, 2007), and the detection of thin snow (<1 cm) is generally problematic for the MODIS sensors overall. The average root mean square error for MODIS fractional snow cover across four mountain ranges is 5%, and retrieval seems to be mostly insensitive to solar zenith angle (Painter et al., 2009). In alpine meadows, where the forest canopy is minimal, MODIS fractional snow cover is almost identical to in situ estimates of snow cover and higher spatial resolution satellite estimates. For example, at high elevation sites in the Tibetan Plateau, MODIS snow cover shows a 90% overall accuracy when related to in situ measurements (Pu et al., 2007). However forest canopies obscure the ground and cause an observed value of snow fraction to be less than true values (Raleigh et al., 2013). MODIS fractional snow cover is used as an input into MODIS albedo (MOD10A1 User Guide) and therefore provides more information about snow cover extent than albedo alone, which integrates information about land covers and snow weathering.

Our objective is to compare monthly MODIS *Average LST*, produced using a non-extrapolating diurnal averaging model, with two types of downscaled air temperature fields for the mountainous southwest Yukon region. We use this comparison between temperature products to evaluate their difference relative to snow cover. The high spatial resolution of MODIS LST and downscaled temperature products are required because trend analysis in areas of large topographical variability is very difficult to interpret at much coarser spatial resolution, typical of passive microwave or re-analysis products that have not been downscaled. The relationships between these datasets were examined for spring and summer 2008 in relation to land cover, elevation, snow cover and number of LST measurements for each month. Lastly we compare the downscaled air temperatures and LST values with nine high elevation meteorological stations that were not used in the production of the datasets examined here.

2. Study area

The southwest Yukon study site (Fig. 1) is bounded by the Yukon – Alaska border on the west (141°W) and southwest, Yukon – British Columbia border on the south (60°N), 138°W on the east and 62°N on the north. The southeast portion of the study area is bounded between the points 60°N, 138°W and 60.3°N, 136.5°W. The northeast side of the study area is bounded between the points 62°N, 141°W and 62.5°N, 138.5°W. The study area, which encompasses 10, 558 2 km by 2 km grid cells, has a large negative west to east elevation gradient of

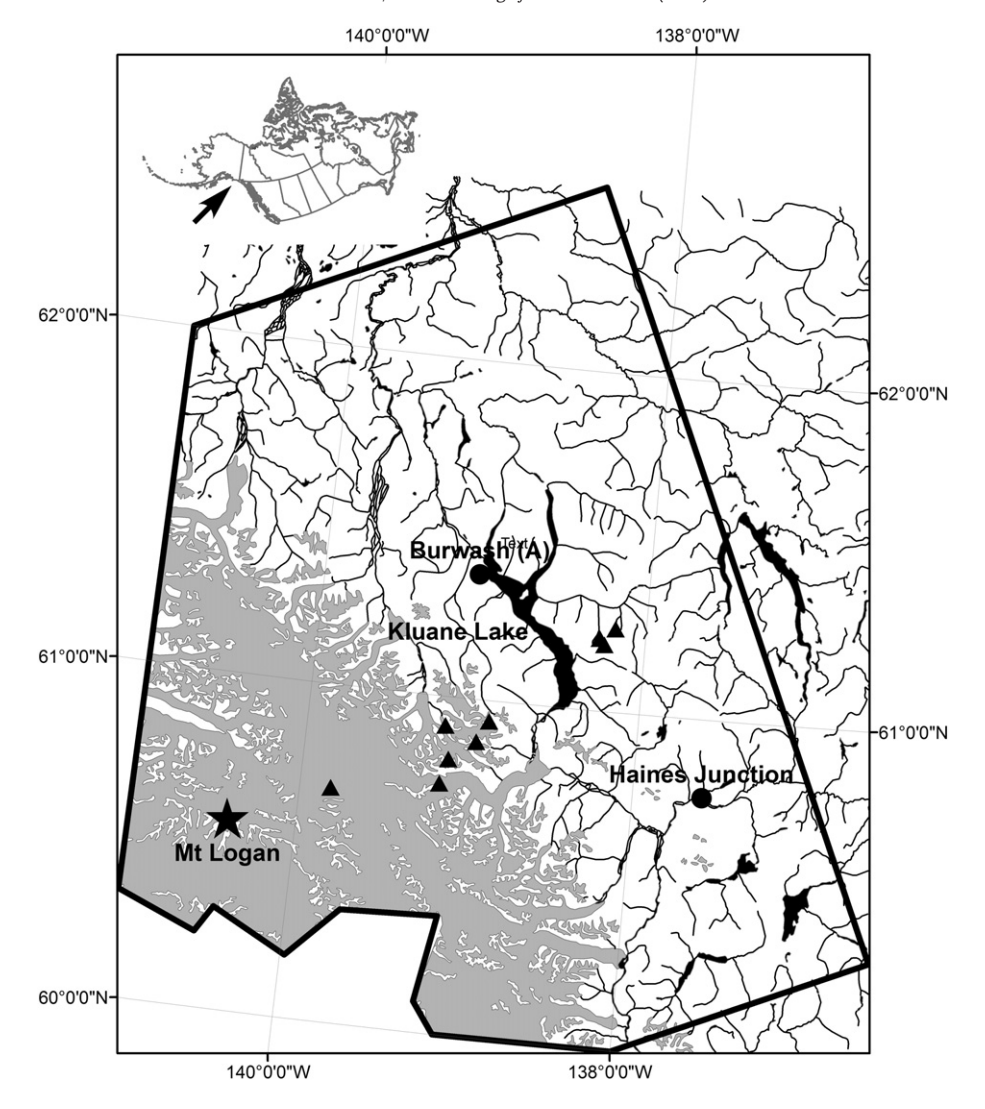


Fig. 1. The southwest Yukon study area bounded by the thick black line. The grey portion is glaciated. The elevational gradient in the study area extends from the summit of Mt. Logan (5959 m) to Kluane Lake (780 m), and some lower elevation drainages. Two Environment Canada meteorological monitoring stations are located within the study area at Haines Junction (655 m) and Burwash Landing (795 m). Nine additional meteorological monitoring stations are found on Permanent Snow & Ice and Sparse Vegetation & Barren land covers (solid triangles).

 $\sim\!5000$ m over $\sim\!120$ km resulting in diverse land-cover types. The 2 km by 2 km grid cells corresponds to the coarsest spatial resolution temperature re-analysis product used in this study. The geographical extent of the study area was chosen to minimise the effect of differences in solar illumination and duration across the longitudinal and latitudinal extent of a MODIS swath, and thus keep the measurements of LST close to solar noon and dawn.

A world-wide landscape classification (GLOBCOVER) was completed in 2009 by the European Space Agency based mainly on MERIS 300 m resolution imagery (http://due.esrin.esa.int/globcover/). Of 23 potential global land cover classes, 11 exist within the study area: Closed needleleaved evergreen forest; Open needleleaved deciduous or evergreen forest; Closed to open mixed broadleaved and needleleaved forest; Mosaic Forest-Shrubland/Grassland; Mosaic Grassland/Forest-Shrubland; Closed to open shrubland; Closed to open grassland; Sparse vegetation; Bare areas; Water bodies; Permanent snow and ice. These classes were reduced by aggregating similar classes in terms of stature and functional type and removing water bodies. The six classes (with areal extent in parentheses) included in the analysis were: 1) Closed and Open needleleaved and needleleaved deciduous forest (6844 km²); 2) Closed to Open mixed broadleaved and needleleaved forest (1956 km²); 3) Mosaic Forest-Shrubland/Grassland - Mosaic Grassland/Forest-Shrubland – Closed to open shrubland (4108 km²); 4) Closed to open grassland (5040 km^2); 5) Sparse vegetation – Bare areas ($13,420 \text{ km}^2$); 6) Permanent snow and ice ($10,268 \text{ km}^2$). These six classes generally increase in average elevation from the conifer dominated class 1 at 936 m, through 1114 m (class 2), 1186 m (class 3), 1165 m (class 4), 1655 m (class 5) and 2325 m (class 6).

Two long-term Environment Canada meteorology monitoring stations are situated at gravel covered airfields at Burwash Landing and Haines Junction within Conifer land cover (Closed and open needleleaved forest) and located at elevations of 806.8 m and 599.0 m, respectively. Data from the Environment Canada stations are integrated into the downscaled temperature products. Nine research meteorological stations (Table 1) are located within the study located between elevations of 1408–2690 m, on Barren or Permanent Snow and Ice land covers and provide hourly air temperature measurements, which were compared to the intersecting temperature product grid cell. The nine stations provide independent validation as none were used in the production of downscaled and satellite temperature products considered in this study.

LST was estimated from radiances measured by the MODIS sensor on the Terra and Aqua platforms. These satellites are in near-polar orbits, which dictate a swath overlap at latitudes >30°, and thus produce progressively more daily observations toward each pole. MODIS data became available in February 2000 for Terra and July 2002 for Aqua. A

Table 1Validation meteorological stations, descriptions and locations.

Site	Location	Description	Station elevation (m)	Grid cell elevation (m)
South Glacier (GL1)	60.82°N, 139.13°W	Permanent Snow & Ice	2280	2427
North Glacier (GL2)	60.91°N, 139.16°W	Sparse Vegetation	2319	2016
Transect Canada Creek	60.88°N, 138.97°W	Sparse Vegetation	2184	2600
Transect Duke River	60.94°N, 138.90°W	Sparse Vegetation	2214	1960
Pika Camp	61.21°N, 138.28°W	Sparse Vegetation	1635	1681
John Creek	61.20°N, 138.25°W	Sparse Vegetation	1408	1812
Ruby Range North	61.25°N, 138.19°W	Sparse Vegetation	1926	1621
Kaskawulsh	60.74°N, 139.17°W	Permanent Snow & Ice	1845	1807
Divide	60.70°N, 139.81°W	Permanent Snow & Ice	2690	2377

full earth sun-synchronous, near-polar orbit for both platforms requires 90 min to complete, with the Terra descending orbit's equatorial crossing at 10:30 AM local time and Aqua's ascending orbit crossing the equator at 1:30 PM local time. The orbitals dictate both Terra and Agua pass over the southwest Yukon during solar noon, whereas Agua also has overpasses before dawn and Terra has overpasses late in the evening. The choice of May through August was determined by the MODIS Agua satellite, because this is the only period where observations coincided with 2 h before dawn to dawn. In the months after August to the winter solstice, the time of dawn occurs progressively later in the day, meaning that the observations by the Agua satellite are occurring earlier than dawn because dawn is occurring later each day. The Terra and Aqua satellite overpasses overlap within 1 h of solar noon in the study area latitudinal and longitudinal range. Using measurements within 1 h of solar noon provides a maximum overpass density, while minimising the daily variability in LST values. Although we call this value maximum LST, it could be less than the actual daily maximum which occurs slightly after solar noon due to phase lag after peak insolation (Jin and Dickinson, 1999). Fig. 2 is a schematic of the MODIS overpass times and the two-hour sampling periods in relation to a generalised clear sky diurnal temperature curve. The position of peak LST will lag behind peak solar insolation depending on surface cover, soil moisture and atmospheric conditions.

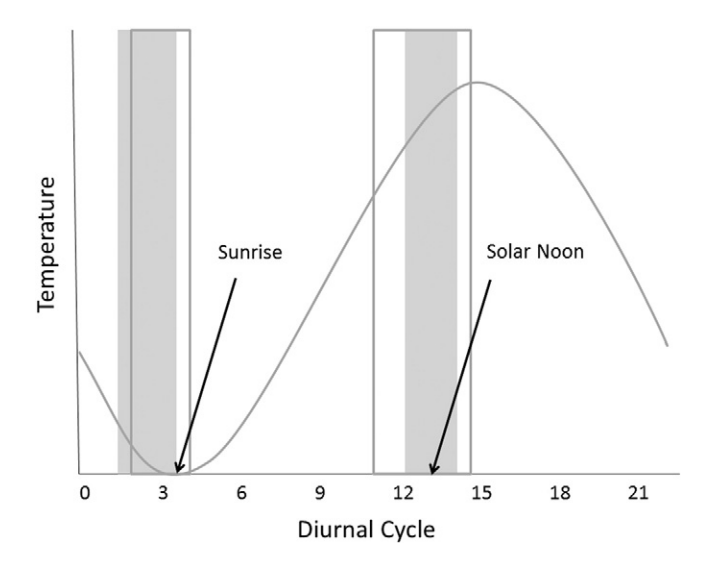


Fig. 2. A generalised diurnal temperature cycle (curve), in the absence of clouds, at the summer solstice (21 June), for the study area in the southwest Yukon. The local times for MODIS overpasses (open boxes) and the two-hour sampling windows (shaded boxes) are shown in relation to sunrise, solar noon and the generalised diurnal temperature curve. Maximum surface skin temperature will occur shortly after solar noon. The open box before sunrise is populated exclusively by MODIS Aqua, whereas the open box covering solar noon is populated by both MODIS Aqua and Terra. The evening MODIS Terra overpasses have been removed for clarity. The positions of the open boxes do not change throughout the year, but the shaded boxes move in relation to intra-annual changes in sunrise and solar noon.

3. Methods

3.1. Processing MODIS data

The MODIS LST data used in this study are the 1 km gridded clearsky reprocessed MODIS Terra and Aqua (MOD11L2 and MYD11L2) LST swath data. The 1 km gridded MODIS LST is produced using the split window technique (Wan et al., 2002; Wan, 2008) that uses MODIS bands 31 and 32 (10.78–11.28 µm and 11.77–12.27 µm respectively). This technique uses a global land surface emissivity derived look-up table (Snyder et al., 1998) to correct for emissivity variability. MODIS data were downloaded from the Land Processes Distributed Active Archive Center - LPDAAC (https://lpdaac.usgs.gov/). The MOD11L2 data are comprised of geolocation, sensor radiance data, atmospheric temperature and water profile, cloud mask, land cover, and snow cover MODIS products. The daytime MODIS LST product has a larger confidence in the daytime cloud mask compared to the night-time mask (Ackerman et al., 1998), which reduces the potential for cloud contamination. The 2008 MYD11L2 and MOD11L2 swath data were reprojected from a sinusoidal projection to 1 km Albers Equal Area Projection (WGS84) using nearest neighbour resampling. This processing step was accomplished using the MODIS Swath Reprojection Tool, run in batch mode, available from the LPDAAC.

The LST was filtered for grid cells that showed anomalous values, caused by cloud or cloud shadow contamination or large view angles (Benali et al., 2012). We adopted an approach similar to that used by Raynolds et al. (2008) on AVHRR LST data for cloud masking of MODIS LST data. If a MODIS LST grid cell was <5 °C than the average of the surrounding values within 2 km radius it was eliminated from analysis. Furthermore if the grid cell temperature was >3 °C different than the surrounding cells average plus standard deviation, it was also eliminated from the analysis.

3.2. Calculating monthly average, maximum and minimum LST

Daily mean LST was calculated as the average of Maximum and Minimum LST and retained the spatial resolution of the input MODIS LST data. Maximum LST was determined (i) by identifying MODIS Aqua and Terra swaths that corresponded to within 1 h before and after solar noon at 61°N and 139.5°W; and (ii) by selecting the maximum value from multiple images for a given day (2 to 4 depending on how the 90 min repeat orbital corresponds to the 2 h interval around solar noon) for each 1 km grid cell. Minimum LST was determined (i) by identifying MODIS Aqua swaths that correspond to the 2 h before dawn. Due to orbital configurations only MODIS Aqua imaged the study area for the two predawn hours; and (ii) by selecting the minimum value for daily images for each 1 km grid cell. Depending on how the satellite repeat orbit of ~90 min corresponds to the two hour predawn interval, 1 to 2 Aqua images were available with which to determine the minimum value. During the remainder of the year at this latitude, dawn occurred too late in the day to coincide with MODIS Aqua coverage. Monthly averages maximum and minimum were calculated from available values,

after which the data were resampled to 2 km grid cells using an arithmetic average.

3.3. MODIS snow cover

Daily snow cover was derived from the MODIS Terra 500 m fractional snow cover (MOD10A1) and resampled to 2 km grid cells using an arithmetic average of the 16 possible values, ignoring missing values. The daily maps of 2 km snow cover were aggregated to monthly averages showing a value of 0–100% for each aggregated grid cell for each month.

3.4. Scenarios Network for Alaska + Arctic Planning (SNAP) air temperature

The SNAP air temperature product applies the delta method of statistical downscaling (Prudhomme et al., 2002) to 1910–2009 CRU data (Climate Research Unit – University of East Anglia) using the 1961–1990 Parameter-Regression on Independent Slopes Model (PRISM) model (Daly et al., 1994) data as the baseline climate. The monthly mean air temperature is gridded at a 2 km resolution for the southwest Yukon.

3.5. North American Regional Re-analysis downscaling

An alternative downscaling method uses an interpolation scheme that reconstructs vertical temperature profiles from a North American Regional Reanalysis (NARR) and does not require meteorological station measurements for tuning. NARR is produced by the National Center for Environmental Prediction (NCEP), and makes use of surface, radiosonde, and satellite data, which are combined in the Eta forecasting system (Mesinger et al., 2006). This method was developed by Jarosch et al. (2012) for western Canada, with the specific intent of producing a temperature product that is more accurate than other products for high elevation, high vertical relief glaciated areas. This product, which is a mix of statistical and dynamical downscaling methods applied to NARR 500 mbar air temperature, uses two-part, piece-wise fitting to NARR vertical air profiles and subsequent interpolation of those fitting parameters to a 200 m grid for prediction of temperature at arbitrary elevation. These data were resampled to 2 km grids using cubic convolution and averaged to monthly time scale. Jarosch et al. (2012) report a mean bias of 0.5 °C for areas with high vertical relief, for the data set encompassing 1990 to 2008. Mean absolute errors of no > 2 °C for monthly averages were found when compared against station temperatures.

3.6. Statistical analyses

All GIS analysis and data manipulation was conducted with ESRI's ArcGIS 10. Statistical analysis and visualisation was conducted using the R statistical software package (R Development Core Team, 2008).

4. Results

May through August 2008 monthly *Average LST* and two downscaled monthly average temperature products for six land cover groups are plotted against snow cover fractions in Fig. 3. The aggregation of temperature products for each land cover type includes only those grid cells where data exists from all three products. The land cover classes are displayed in decreasing average elevation (top to bottom), where the Permanent Snow & Ice cover class is located at the top of the elevation set. The temperature measures, displayed as a function of snow cover, increased from May to July and then decreased in August. As expected, the snow fractions in the Permanent Snow & Ice class decrease from May to July as snow melting exposed bare ground. For the low elevation classes, where permanent snow and ice are not present, the maximum snow cover fraction decreases from ~50–70% in May toward the July minimum. Downscaled air temperatures overlap, or are very

close to, the Average LST values plus or minus standard error, for snow fractions < 10% in the Conifer land cover class (where the Environment Canada meteorological stations are situated). The two downscaled products show a very similar negative relationship between temperature and snow cover with an offset between them for high elevation Permanent Snow & Ice and Sparse and Barren classes. The SNAP temperature product does not display this strong negative relationship for the rest of the lower elevation land cover classes. The statistically downscaled SNAP temperature product is consistently warmer than the downscaled NARR product. The monthly average of daily MODIS fractional snow cover that intersect the Environment Canada meteorological stations at Burwash Landing and Haines Junction ranges between 0% and 0.48% for the study period. The exception to this range occurs for Burwash Landing for August where the snow cover fraction is 1.7%. The very small snow cover fractions that occur at the meteorological stations suggest that unrepresentative, warmer temperatures are being interpolated to obtain temperatures for higher elevation snow covered sites with the SNAP product.

Average LST (Fig. 3) is consistently and progressively colder than SNAP and NARR temperatures averages for snow fractions greater than ~40%. The land cover classes covered by large snow fractions (>90%) display average LST temperatures 5–7 °C colder than the downscaled temperature products. The difference between downscaled NARR temperatures and average LST is smaller than that of downscaled SNAP and closer in absolute values. Inspection of the Permanent Snow & Ice and the Sparse Vegetation & Barren classes indicate that the difference between average LST and the downscaled interpolated products increases slightly from May to August. Fig. 4 displays monthly Average Maximum LST in relation to SNAP and NARR monthly averages by snow fraction. Fig. 5 shows monthly Average Minimum LST. Maximum monthly average LST displays a large decrease in temperature by ~20 °C over the range of snow covers from 10% to 100%. At the 80%– 100% range of snow cover, the maximum LST has values slightly below 0 °C, and tends to be similar to the downscaled temperature products. Minimum monthly average LST is uniformly colder than the downscaled products by ~10 °C for all snow cover fractions.

Table 2 shows the average number of monthly maximum and minimum LST observations and standard deviation within a month for each 10% category of snow cover for each point in Figs. 4 and 5. The number of monthly maximum LST measurements is roughly stable across all four months and varies between 2.2 and 11.8 with an average of 5.5. The number of monthly minimum LST measurements varies considerably by land cover (elevation) and month and ranges between 3.1 and 14.0 with an average of 8.4. For the higher elevation ground covers, in May and August, the number of minimum measurements of LST outnumbers maximum by approximately 2–3 times. The numbers of maximum and minimum LST measurements becomes much closer in number in the Conifer land cover. The number of minimum LST measurements in June and July is approximately half of May and August.

Intersecting grid cells for the three monthly average temperature products are compared with all sky air temperature measured at nine meteorological stations (Table 1) not used in the generation of any of the products. The results are found in Table 3. The stations are located on Barren, Sparsely Vegetated or Permanent Snow & Ice land cover types. The SNAP and NARR downscaled temperatures are typically within ± 2 °C of the air temperature average irrespective of differences between station elevation and the intersecting grid cell average elevation. In contrast, the grid cells with <10% snow cover displayed an average LST of 1-3 °C warmer than the other measures of temperature and grid cells with >90% snow cover displayed an average LST of 4–6 °C colder than the other measures of temperature. Table 4 provides the Root Mean Square Error and Bias between NARR, SNAP and LST compared to the meteorological stations outlined in Table 1. The RMSE was <2.5 °C for snow fractions of <40% when compared to station air temperature for all three average temperature products; the Bias for these products was < 2.0 °C.

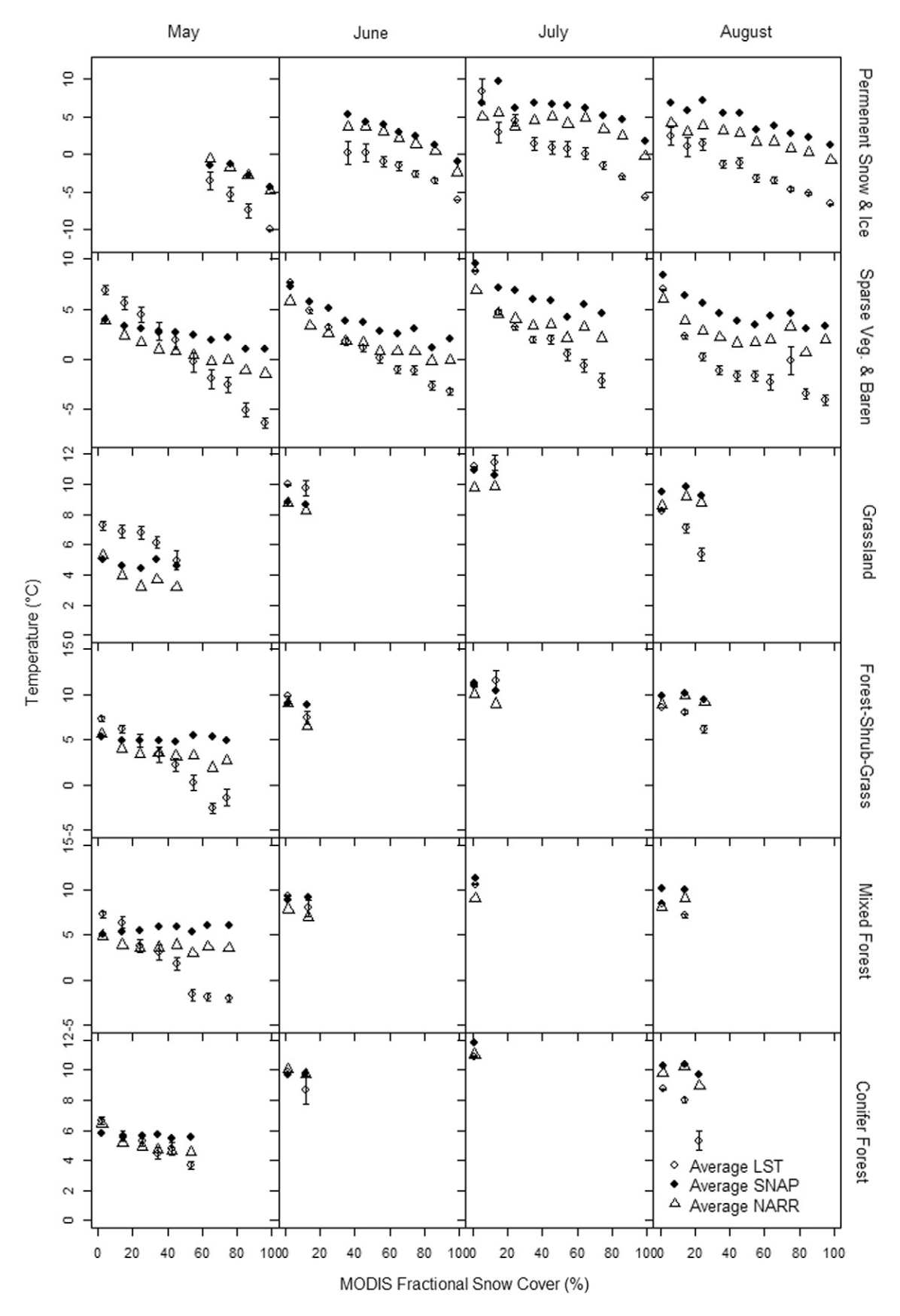


Fig. 3. MODIS Average Land Surface Temperature (LST) compared to downscaled interpolated air temperature (SNAP) and downscaled NARR temperature plotted against snow fractions in 10% bins, for May through August 2008 monthly means. Six aggregated land cover classes decrease in elevation from top Permanent Snow and Ice to bottom Conifer forest. Error bars indicate standard error for MODIS LST. Standard error for SNAP and NARR has been removed for clarity, but in general is less than the symbol size.

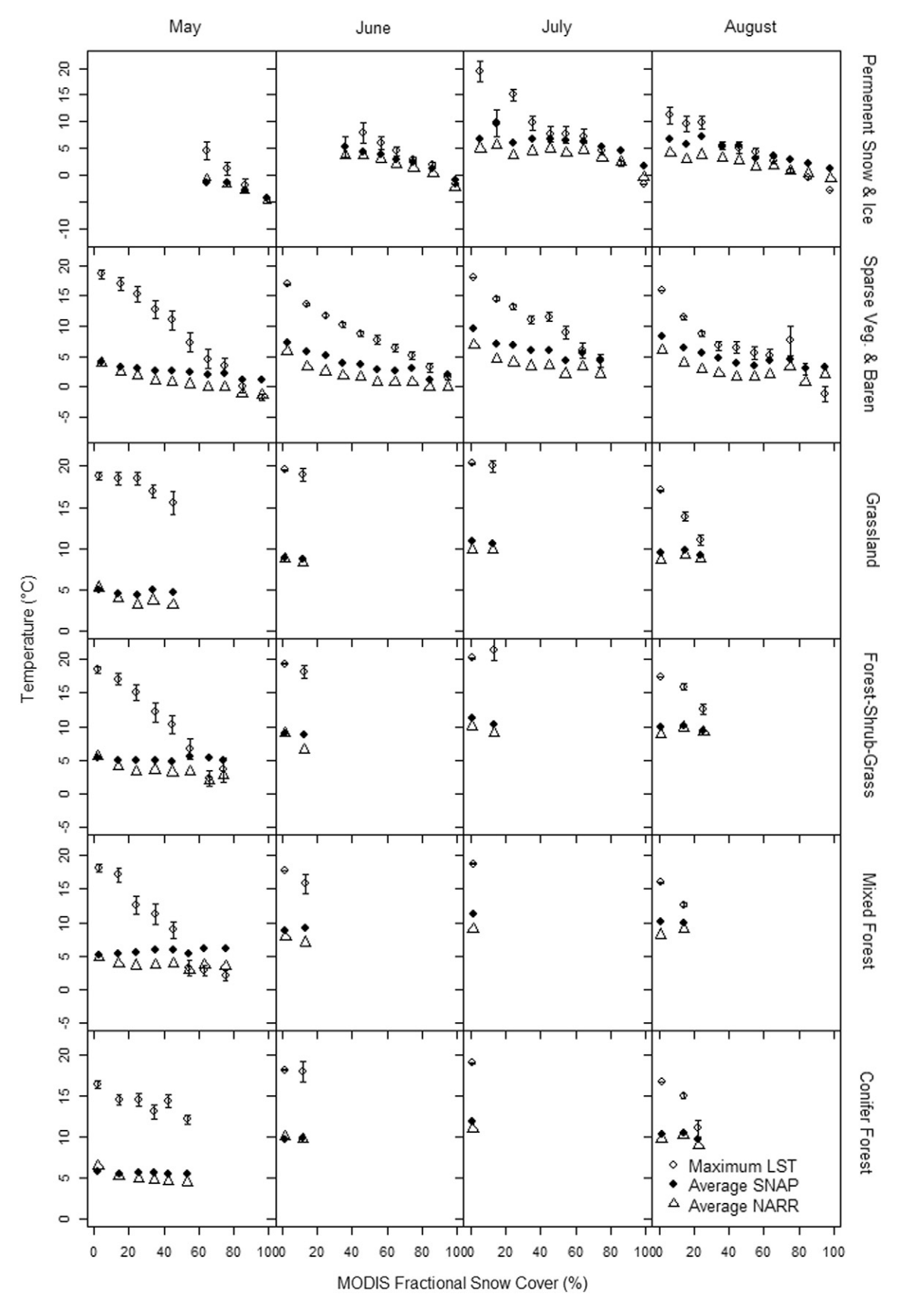


Fig. 4. MODIS *Maximum Land Surface Temperature* (LST) compared to downscaled interpolated air temperature (SNAP) and downscaled NARR temperature plotted against snow fractions in 10% bins, for May through August 2008 monthly means. Six aggregated land cover classes decrease in elevation from top Permanent Snow and Ice to bottom Conifer forest. Error bars indicate standard error for MODIS LST. Standard error for SNAP and NARR has been removed for clarity, but in general is less than the symbol size.

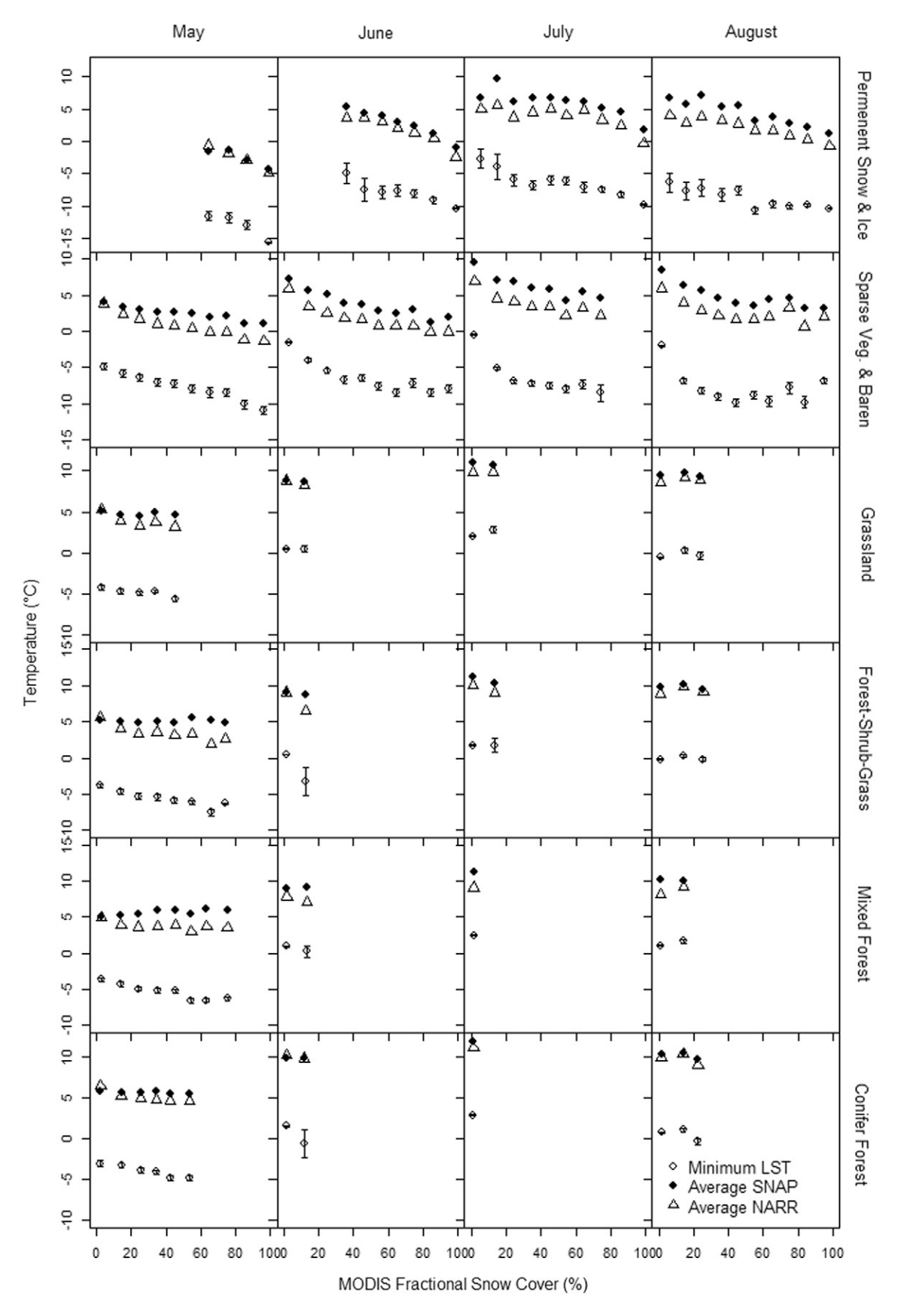


Fig. 5. MODIS Minimum Land Surface Temperature (LST) compared to downscaled interpolated air temperature (SNAP) and downscaled NARR temperature plotted against snow fractions in 10% bins, for May through August 2008 monthly means. Six aggregated land cover classes decrease in elevation from top Permanent Snow and Ice to bottom Conifer forest. Error bars indicate standard error for MODIS LST. Standard error for SNAP and NARR has been removed for clarity, but in general is less than the symbol size.

Table 2The average number of daily observations of maximum and minimum LST for each month and 10% snow cover bins. Standard deviation for the number of observations in each 10% snow cover bin is also included. This table is presented with the same categories as Fig. 3.

Land cover	Snow	•				June	June Ju				July				August		
	cover	Max Obs	Max Sd	Min Obs	Min Sd	Max Obs	Max Sd	Min Obs	Min Sd	Max Obs	Max Sd	Min Obs	Min Sd	Max Obs	Max Sd	Min Obs	Min Sd
Permanent Snow & Ice	<10%									6.6	1.6	5.4	0.7	5.3	3.0	9.6	2.3
	10%-20%									4.6	2.1	6.7	1.9	5.1	3.0	10.4	4.7
	20%-30%									3.3	1.3	7.6	3.1	4.6	1.8	10.1	3.0
	30%-40%					4.8	5.2	6.9	2.3	5.0	3.7	7.7	2.8	5.0	3.7	11.1	3.5
	40%-50%					7.4	6.5	6.5	2.5	4.1	3.1	8.0	2.9	3.9	2.6	10.9	4.0
	50%-60%					5.4	2.6	5.9	2.7	3.3	2.1	6.9	3.5	3.8	2.6	12.5	3.4
	60%-70%	4.5	3.6	12.8	3.0	3.4	2.3	5.8	2.4	3.9	2.8	8.1	3.0	3.5	2.3	11.5	3.7
	70%-80%	4.1	2.3	12.3	2.2	3.7	2.8	6.2	2.7	3.0	2.1	8.7	4.0	3.1	1.9	12.2	3.5
	80%-90%	4.5	2.9	13.2	2.4	3.1	1.9	6.4	2.6	3.2	2.0	7.5	3.7	3.6	2.0	11.3	3.5
	>90%	8.4	3.3	11.8	2.6	5.0	2.5	6.4	2.4	3.7	1.9	7.1	3.0	5.6	2.6	9.4	3.2
Sparse Vegetation & Barren	<10%	7.8	4.8	10.9	1.8	7.7	3.1	4.9	1.8	7.6	2.5	5.7	1.9	7.4	2.8	7.5	2.5
	10%-20%	6.0	4.5	11.5	2.0	6.4	3.7	5.4	2.1	5.7	3.0	7.0	2.5	6.4	3.3	10.5	3.8
	20%-30%	5.5	4.4	12.0	2.0	5.4	3.5	5.6	2.0	5.7	2.9	8.0	2.8	5.9	3.3	11.7	3.4
	30%-40%	4.2	3.4	12.0	2.0	5.0	3.1	5.8	2.2	4.2	2.4	8.9	3.0	4.8	3.0	12.3	3.9
	40%-50%	4.1	2.9	12.3	2.1	4.0	3.0	6.4	2.0	4.5	3.2	8.2	2.9	4.4	2.9	12.9	3.8
	50%-60%	4.1	2.9	12.5	2.1	4.4	3.6	6.6	2.5	3.1	1.9	8.4	3.0	3.6	2.2	11.9	3.0
	60%-70%	4.3	2.9	12.8	2.1	4.2	2.4	6.7	2.6	3.7	3.1	8.3	3.3	5.1	3.3	13.2	3.5
	70%-80%	4.2	2.4	12.5	2.2	3.4	2.5	7.1	2.3	2.2	1.0	8.1	5.0	4.0	5.3	11.5	3.5
	80%-90%	4.4	2.4	12.8	2.2	2.8	1.4	7.8	3.3					3.5	1.3	14.0	1.8
Clared to a second and	>90%	6.0	3.1	12.9	2.4	3.7	1.9	7.7	2.9	7.5	2.0	F 2	17	4.9	2.2	6.3	1.2
Closed to open grassland	<10% 10%–20%	8.9 6.2	3.5 3.1	10.4 11.2	1.9 2.0	7.9 6.8	2.4 2.8	4.4 5.0	1.6 1.9	7.5 6.2	2.0 0.9	5.3 4.5	1.7 1.0	6.9 6.7	1.9 2.2	5.5	2.1
	20%-30%		2.3		2.0 1.9	0.8	2.8	5.0	1.9	6.2	0.9	4.5	1.0	5.7	1.5	5.4	1.7
		5.0 5.0		11.3										5.7	1.5	4.3	1.1
	30%-40% 40%-50%	5.0	2.7 2.4	12.4 12.7	1.6 2.0												
Mosaic Forest, Shrubland,		5.0 10.0	3.4	10.4	2.0 1.9	0.4	2.7	4.4	1.7	7.8	2.0	5.1	1.7	7.5	2.2	6.3	2.1
Grassland	<10% 10%–20%		3.4		2.4	8.4 5.0	2.7 2.7	3.8	2.0	6.0	3.0	5.1	1.7	7.5 7.6	1.4	4.8	
Glassialiu	20%-30%	6.1 4.7	2.9	11.1 12.1	1.7	5.0	2.7	5.0	2.0	0.0	5.0	5.4	1.0	7.6 5.4	1.4	4.6	1.2 1.3
	30%-40%	6.0	2.5	11.8	1.7									3.4	1,2	4.0	1.5
	40%-50%	5.0	2.6	12.3	1.7												
	50%-60%	5.2	2.0	12.7	1.5												
	60%-70%	3.9	2.9	11.7	1.8												
	70%-80%	4.9	1.7	13.0	1.3												
Mixed forest	<10%	8.0	3.3	10.0	2.1	8.3	2.9	4.6	1.7	7.6	1.9	4.9	1.6	7.1	2.2	6.3	1.9
Wince forest	10%-20%	5.1	2.5	11.4	2.2	4.7	2.1	4.1	1.6	7.0	1.5	4.5	1.0	7.4	1.5	5.2	1.1
	20%-30%	4.8	2.6	12.0	2.2	1.7	2.1	1.1	1.0					,,,	1.5	3.2	1.1
	30%-40%	4.8	2.1	12.6	1.9												
	40%-50%	5.1	2.0	12.4	1.7												
	50%-60%	3.3	1.3	11.9	1.7												
	60%-70%	3.9	1.5	11.3	2.1												
	70%-80%	4.7	1.2	11.6	1.5												
Conifer forest	<10%	11.8	3.3	9.8	2.0	10.1	3.1	4.3	1.7	9.3	2.3	5.4	1.6	8.7	2.4	6.4	2.2
	10%-20%	10.2	3.6	11.1	2.2	7.3	5.0	3.1	1.2	0.5				7.7	2.1	5.2	1.5
	20%-30%	9.1	4.7	11.6	2.3		0.0	J.,						6.2	0.9	4.3	1.0
	30%-40%	9.5	3.5	12.7	2.2									0.2	0.0		
	40%-50%	7.8	2.5	12.4	1.5												
	50%-60%	9.3	3.5	12.9	1.0												

These values compare well with the RMSE for other studies on LST (e.g., André et al., 2015). For snow fractions of >40%, the Bias is $-4.5\,^{\circ}$ C, and the RMSE is 6.1 °C, whereas the downscaled products Bias and RMSE are similar for the <40% snow fraction comparisons. The comparison of Maximum LST to monthly average air temperature shows a large positive Bias for <40% snow fraction, but almost no Bias for >40%. A large negative Bias for both snow fraction categories is displayed against average air temperature for Minimum average LST. Both Maximum and Minimum LST display large RMSE when compared against average air temperature, as expected.

5. Discussion

Accurate LST or 'skin temperature' estimation is critical for improving estimates of surface water, energy, and radiation balance, atmospheric temperature and humidity profiles, with the objective of improving weather and climate forecast accuracy (Reichle et al., 2010). It is well understood that there are biases in how various satellite and modeled estimates compare with ground-based observations, and

the accuracy of temperature trends depends on how well we understand how these products are related. In terrestrial landscapes dominated by seasonal snow cover understanding these relationships are critical for improved understanding of feedback processes associated with Artic amplification (Serreze et al., 2009) and elevation dependent warming (Pepin et al., 2015). Similarly, in polar oceans, Kang et al. (2015) reported that systematic temperature disagreement associated with surface type classification had an impact on the resulting temperature trends.

In our study, we observed that downscaled air temperature, station air temperature, and Average LST all grow progressively colder as the snow fraction increases for high elevation land covers. Snow exhibits a high albedo, which tends to cool the surface compared to air temperature and thus partially explains why difference between LST and air temperature is larger over snow covered areas. For grid cells with partial snow cover (<40%) the Average LST tends to be warmer than downscaled temperatures. The trend in average LST is largely caused by the strong decline in Maximum LST, to ~0 °C as snow fractions get larger, coupled with the uniformly cold minimum LST values. Thus maximum LST is a better indicator of snow cover change than is Minimum LST.

Table 3
The comparison of air temperature from nine meteorological stations to the temperature values of intersecting NARR, SNAP and LST (Average, Maximum and Minimum) grid cells. Included is the number of observations of Minimum and Maximum LST. NA refers to LST grid cells where Average LST could not be calculated because Minimum or Maximum LST was not acquired.

Month	Site	Snow cover (%)	Station Tair (°C)	NARR (°C)	SNAP (°C)	LST Ave (°C)	LST Max (°C)	LST Max Obs	LST Min (°C)	LST Min Obs
May	South Glacier (GL1)	99.5	-3.8	-5.3	-3.6	-12.1	-8.2	2.7	-16.1	13.5
	North Glacier (GL2)	79.4	-3.5	-2.7	-3.8	NA	NA	NA	NA	NA
	Transect Canada Creek	98	-2.2	-5.3	-4.1	-13.1	-9.4	5.7	-16.9	16.2
	Transect Duke River	89.6	-3.9	-2.3	-2.8	-9.1	-3.9	6.2	-14.3	18.3
	Pika Camp	61.2	0.4	1.7	1.1	7.5	20.8	2.5	-5.8	11.7
	Kaskawulsh	99.1	-1.5	-1.4	1.0	NA	NA	NA	NA	NA
	Divide	99.5	-7.9	-5.6	-5.7	-10.3	-4.2	12.5	-16.4	15.8
June	South Glacier (GL1)	98.0	0.0	-2.4	0.2	NA	NA	NA	NA	NA
	North Glacier (GL2)	71.5	0.2	0.6	1.2	-2.6	3.3	2.5	-8.5	11.0
	Transect Canada Creek	61.8	1.0	-2.3	-0.4	-6.1	-1.2	2.0	-11.1	9.0
	Transect Duke River	66.7	0.0	1.0	1.1	1.2	7.7	3.3	-5.2	9.3
	Pika Camp	3.4	3.9	4.7	5.3	6.7	14.7	8.3	-1.3	5.8
	Kaskawulsh	95.3	2.7	1.8	3.9	-2.2	0.8	5.3	-5.1	8.5
	Divide	100	-3.7	-2.8	-1.5	-6.3	-0.9	3.5	-11.8	4.8
July	South Glacier (GL1)	41.9	1.2	2.8	3.0	NA	NA	NA	NA	NA
	North Glacier (GL2)	72.4	1.8	0.1	3.2	NA	NA	NA	NA	NA
	Transect Canada Creek	88.1	2.7	0.2	3.4	NA	NA	NA	NA	NA
	Transect Duke River	20.8	1.9	3.2	4.1	1.0	11.4	5.0	-9.5	9.8
	Pika Camp	0.0	5.6	6.3	8.2	9.0	17.8	7.8	0.2	3.5
	Kaskawulsh	86.0	4.4	4.0	6.7	-1.0	6.4	3.3	-8.5	4.8
	Divide	99.9	-2.1	-0.1	1.9	-6.0	-1.3	3.3	-10.7	4.8
August	South Glacier (GL1)	70.2	0.9	2.4	-0.3	-5.5	-2.6	2.7	-8.5	12.5
	North Glacier (GL2)	32.1	1.1	3.5	2.2	2.2	13.4	4.2	-8.9	15.0
	Transect Canada Creek	64.2	2.1	2.0	-0.4	-6.6	-2.7	2.2	-10.5	16.7
	Transect Duke River	10.5	1.4	3.5	2.5	3.5	12.1	4.2	-5.1	11.7
	Pika Camp	0.0	4.6	7.3	5.5	7.3	15.2	10.5	-0.6	4.2
	John Creek	0.0	5.5	7.0	4.6	6.8	16.1	8.5	-2.6	6.0
	Ruby Range North	0.0	2.9	7.3	5.1	6.6	15.4	9.5	-2.2	5.5
	Kaskawulsh	82.1	3.7	7.8	3.6	-3.1	-0.3	5.0	-5.8	9.2
	Divide	99.4	-2.3	1.2	-0.3	-6.2	-3.8	8.5	-8.7	10.8

We expected the LST averages to be within 2–3 °C (Root Mean Square Deviation) of air temperature for snow-free vegetated surfaces (Zaksek and Schroedter-Homscheidt, 2009) or when using daytime temperature measurements exclusively over snow covered terrain (Hall et al., 2008). An analysis by Williamson et al. (2013) showed that near-instantaneous matching of daytime MODIS LST and air temperature for conifer forests is highly correlated throughout the year for the two Environment Canada meteorological stations in the study area. The high correlation is very likely because the daytime clear sky MODIS LST measurements are for the conifer forest canopy top, which conceals snow covered ground. Night-time measurements were not investigated.

Westermann et al. (2012) showed that the inclusion of Minimum LST into longer term averages caused a cold bias compared to in-situ ground level measurements of skin temperature of between 1.5 and 6 °C, with a mean bias of 3 °C, in winter Svalbard, which agrees with the results shown here. Cloud cover increases the average minimum skin temperature, compared to the clear sky satellite measurement of MODIS LST, and is the reported cause of the discrepancy. This phenomenon is also seen when making aggregated eight-day averages using

Table 4The RMSE and BIAS of the monthly NARR, SNAP and LST (Average, Maximum and Minimum) grid cells which intersect with the meteorological station air temperatures presented in Table 3. The RMSE and BIAS were calculated for two groups of snow cover percentage from the meteorological grid cell and for the measurements encompassing all the snow cover fractions.

Snow cover (%)	NARR (°C)		SNAP (°C)		LST Average (°C)		LST Maximum (°C)		LST Minimum (°C)	
	RMSE	BIAS	RMSE	BIAS	RMSE	BIAS	RMSE	BIAS	RMSE	BIAS
<40	2.3	2.0	1.7	1.3	2.5	2.0	11.2	11.1	7.5	-7.1
>40	2.1	0.6	1.8	0.7	6.1	-4.5	6.3	0.7	9.9	-9.6
All	2.2	1.0	1.8	0.9	5.1	-2.3	8.3	4.2	9.2	-8.8

Minimum and Maximum LST gathered from the same day or from different days within the same eight-day period (Williamson et al., 2014). However we observed that the number of monthly measurements of Maximum and Minimum temperatures seems to exert little influence on the relationship between downscaled air temperature and Average LST. This was confirmed by comparing the number of observations of Maximum or Minimum LST (Table 2) to the trends in downscaled temperatures compared to Maximum and Minimum LST (Figs. 4 and 5). If the number of observations was playing a large role in determining the discrepancy between downscaled air temperature and LST, then the difference between these measures of temperature should be governed by the number of observations, which was not observed. Our results indicate that the effect found by Westermann et al. (2012) also operates in summer (as it does in winter), but only for snow fractions greater than ~40%. The opposite relationship occurs in summer when the snow fraction is less than ~10% in a grid cell: average LST is greater than air temperature for land cover classes above treeline. This is caused by a clear sky bias to warm temperatures for maximum values of LST. Cloud cover trends can make the interpretation of clear sky remote sensing measurements of skin temperature with all sky air temperature trends difficult (Westermann et al., 2012; Østby et al., 2014). Snow cover, and more importantly snow cover changes, should also be considered when conducting trend analysis of skin temperatures, especially at high elevation, where high spatial resolution LST is a valuable data source.

Several areas require further work to fully clarify the relationships we observed between downscaled air temperature products and LST with regard to snow and cloud cover. Improved fractional snow cover algorithms for MODIS will provide an increased level of confidence in the corrections required for temperature products, especially in densely forested land covers or areas of high vertical relief. The relationship between Maximum and Minimum LST in relation to other temperature products can aid in the investigation of atmospheric and ground heat fluxes (i.e., surface energy balance, which can help understand

surface-atmosphere feedbacks), especially in remote areas experiencing snow cover change. Finally, the relationship between cloud cover and snow cover needs further exploration in relation to decadal temperature trends.

6. Conclusions

We used the four summer months of 2008 to assess the relationship between downscaled air temperature and average LST and the variation in these relationships caused by differences in snow cover. We find that summer 'clear sky' satellite derived infrared skin temperature has a cold bias in Average LST because of the interplay between Minimum and Maximum LST over different land cover types, but only when there is snow cover greater than ~40%. Average LST is 5-7 °C colder than both the downscaled and observational temperature products for >90% snow covered grid cells. Furthermore, for maximum LST converges with average air temperature for high snow cover fractions. Conversely, average LST is 1–3 °C warmer for grid cells with snow cover < 10%. Both of these findings are confirmed from independent meteorological measurements of air temperature from within the study area. These findings indicate that analysis of snow cover should occur in conjunction with statistical analysis of time series of LST, especially in high latitude and high elevation locations where validation is difficult. Systematic comparison of LST to downscaled air temperature can provide insight into the dynamic surface energy balance in this complex, changing landscape.

Acknowledgements

Financial support for this project was provided by the Canada Foundation for Innovation, the Canada Research Chairs Program, the Government of Canada International Polar Year Program (PPS Arctic Canada Project), NSERC (Discovery and International Polar Year Programs), the Northern Scientific Training Program (AANDC), and the Canadian Circumpolar Institute at the University of Alberta. G. Flowers and C. Zdanowicz provided additional meteorological data. We thank an anonymous reviewer for helpful comments which improved the manuscript.

References

- Arctic Climate Impact Assessment (ACIA) Report, 2005. Impacts of a Warming Arctic. Cambridge University Press, UK (146 p.).
- Ackerman, S.A., Strabala, K.I., Menzel, W.P., Frey, R.A., Moeller, C.C., Gumley, L.E., 1998. Discriminating clear sky from clouds with MODIS. J. Geophys. Res. 103, 32141–32157.
- AMAP (Arctic Monitoring and Assessment Programme), 2011. SWIPA Overview Report. In: Shearer, R., Wrona, F., Klint, M., Larsen, H., Skovgaard, O., Mahonen, O., Jensson, H., Dovle, P., Tsaturov, Y., Lundeberg, T., Armstrong, T., Solbakken, J.-I. (Eds.), Changes in Arctic Snow, Water, Ice and Permafrost. SWIPA 2011 Overview Report. Arctic Monitoring and Assessment Programme (AMAP) Oslo. xi + 97pp.
- André, C., Ottlé, C., Royer, A., Maignan, F., 2015. Land surface temperature retrieval over circumpolar Arctic using SSM/I-SSMIS and MODIS data. Remote Sens. Environ. 162, 1–10.
- Benali, A., Carvalho, A.C., Nunes, J.P., Carvalhais, N., Santos, A., 2012. Estimating air surface temperature in Portugal using MODIS LST data. Remote Sens. Environ. 124, 108–121. Comiso, J.C., 2003. Warming trends in the Arctic from clear sky satellite observations. J. Clim. 16, 3498–3510.
- Daly, C., Neilson, R.P., Phillips, D.L., 1994. A statistical-topographical model for mapping climatological precipitation over mountainous terrain. J. Appl. Meteorol. 33, 140–158.
- Hall, D.K., Box, J.E., Casey, K.A., Hook, S.J., Shuman, C.A., Steffen, K., 2008. Comparison of satellite-derived and in-situ observations of ice and snow surface temperatures over Greenland. Remote Sens. Environ. 112, 3739–3749.
- Hall, D.K., Riggs, G.A., 2007. Accuracy assessment of the MODIS snow products. Hydrol. Process. 21, 1534–1547.
- Hall, D.K., Riggs, G.A., Salomsonson, V.V., DiGirolamo, N.E., Bayd, K.J., 2002. MODIS snow-cover products. Remote Sens. Environ. 83, 181–194.
- Jarosch, A.H., Anslow, F.S., Clarke, G.K.C., 2012. High-resolution precipitation and temperature downscaling for glacier models. Clim. Dyn. 38. http://dx.doi.org/10.1007/s00382-010-0949-1.
- Jin, M., Dickinson, R.E., 1999. Interpolation of surface radiative temperature measured from polar orbiting satellites to a diurnal cycle: 1. Without clouds. J. Geophys. Res.-Atmos. 104. http://dx.doi.org/10.1029/1998JD200005.

- Jin, M., Dickinson, R.E., 2010. Land surface skin temperature climatology: benefitting from the strengths of satellite observations. Environ. Res. Lett. 5. http://dx.doi.org/10.1088/ 1748-9326/4/044004.
- Kang, H.-J., Yoo, J.-M., Jeong, M.-J., Won, Y.-I., 2015. Uncertainties of satellite-derived surface skin temperatures in the polar oceans: MODIS, AIRS/AMSU, and AIRS only. Atmos. Meas. Tech. 8:4025–4041. http://dx.doi.org/10.5194/amt-8-4025-2015.
- Mesinger, F., DiMego, G., Kalnay, E., Mitchell, K., Shafran, P.C., Ebisuzaki, W., Jović, D., Woollen, J., Rogers, E., Berery, E.H., Ek, M.B., Fan, Y., Grumine, R., Higgins, W., Li, H., Lin, Y., Manikin, G., Parrish, D., Shi, W., 2006. North American Regional Reanalysis. Bull. Am. Meteorol. Soc. 87, 343–360.
- Muster, S., Langer, M., Abnizova, A., Young, K.L., Boike, J., 2015. Spatio-temporal sensitivity of MODIS land surface temperature anomalies indicates high potential for large-scale land cover change detection in Arctic permafrost landscapes. Remote Sens. Environ. 168, 1–12
- Oke, T.R., 1987. Boundary Layer Climates. 2nd edn. Methuen, London.
- Østby, T.I., Schuler, T.V., Westermann, S., 2014. Severe cloud contamination of MODIS Land Surface Temperature over an Arctic ice cap, Svalbard. Remote Sens. Environ. 142, 95–102.
- Painter, T.H., Rittger, K., McKenzie, C., Slaughter, P., Davis, R.E., Dozier, J., 2009. Retrieval of subpixel snow covered area, grain size, and albedo from MODIS. Remote Sens. Environ. 113. 868–879.
- Pepin, N., Bradely, R.S., Diaz, H.F., Baraer, M., Caceres, E.B., Forsythe, N., Fowler, H., Greenwood, G., Hasmi, M.Z., Liu, X.D., Miller, J., Ning, L., Ohmura, A., Palazzi, E., Rangwala, I., Schoener, W., Severskiy, I., Shahgedanova, M., Williamson, S.N., Yang, D.Q., 2015. Elevation-dependent warming in mountain regions of the world. Nat. Clim. Chang. 5, 424–430.
- Prudhomme, C., Reynard, N., Crooks, S., 2002. Downscaling of global climate models for flood frequency analysis: where are we now? Hydrol. Process. 16, 1137–1150.
- Pu, Z., Xu, L., Salomonson, V., 2007. MODIS/Terra observed seasonal variations of snow cover over the Tibetan Plateau. Geophys. Res. Lett. 34, L06706. http://dx.doi.org/10. 1029/2007GL029262.
- R Development Core Team, 2008. R: A Language and Environment for Statistical Computing. R Foundation for Statistical Computing. (Vienna, Austria). (ISBN 3-900051-070-0, URL http://www.R-project.org).
- Raleigh, M.S., Rittger, K., Moore, C.E., Henn, B., Lutz, J.A., Lundquist, J.D., 2013. Ground-based testing of MODIS fractional snow cover in subalpine meadows and forest of the Sierra Nevada. Remote Sens. Environ. 128, 44–57.
- Raynolds, M.K., Comiso, J.C., Walker, D.A., Verbyla, D., 2008. Relationship between satellite-derived land surface temperatures, arctic vegetation types, and NDVI. Remote Sens. Environ. 112, 1884–1894.
- Reichle, R.H., Kumar, S.V., Mahanama, S.P.P., Koster, R.D., Liu, Q., 2010. Assimilation of satellite-derived skin temperature observations into land surface models. J. Hydrometeorol. 11, 1103–1122.
- Robeson, S.M., 1995. Resampling of network-induced variability in estimates of terrestrial air temperature change. Clim. Chang. 29, 213–229.
- Royer, A., Poirier, S., 2010. Surface temperature spatial and temporal variations in North America from homogenized satellite SMMR-SSM/I microwave measurements and reanalysis for 1979–2008. J. Geophys. Res. 115, D08110. http://dx.doi.org/10.1029/ 2009ID012760.
- Salomonson, V.V., Appel, I., 2004. Estimating fractional snow cover from MODIS using the normalised difference snow index. Remote Sens. Environ. 89, 351–360.
- Sellers, W.D., 1965. Physical Climatology. Univ. of Chicago Press, Chicago, Il (272 p.).
- Serreze, M., Barrett, A., Stroeve, J., Kindig, D., Holland, M., 2009. The emergence of surface-based Arctic amplification. Cryosphere 3, 11–19.
- Snow, Water, Ice, Permafrost in the Arctic (SWIPA) (2011) (Accessed 22 April 2013, http://amap.no/swipa).
- Snyder, W.C., Wan, Z., Zhang, Y., Feng, Y.Z., 1998. Classification-based emissivity for land surface temperature measurement from space. Int. J. Remote Sens. 19, 2753–2774.
- Vincent, L.A., Mekis, E., 2006. Changes in daily and extreme temperature and precipitation indices for Canada over the twentieth century. Atmosphere-Ocean 44, 177–193.
- Wan, Z., Zhang, Y., Zhang, Q., Li, Z., 2002. Validation of the land-surface temperature product retrieved from Terra Moderate Resolution Imaging Spectroradiometer data. Remote Sens. Environ. 83, 163–180.
- Wan, Z., 2008. New refinements and validation of MODIS land-surface temperature/emissivity products. Remote Sens. Environ. 112, 59–74.
- Westermann, S., Langer, M., Boike, J., 2012. Systematic bias of average winter-time land surface temperatures inferred from MODIS at a site on Svalbard, Norway. Remote Sens. Environ. 118, 162–167.
- Westermann, S., Østby, T.I., Gisnås, K., Schuler, T.V., Etzelmüller, B., 2015. A ground temperature map of the North Atlantic permafrost region based on remote sensing and reanalysis data. Cryosphere 9, 1303–1319.
- Williamson, S.N., Hik, D.S., Gamon, J.A., Kavanaugh, J.L., Koh, S., 2013. Evaluating the quality of clear-sky MODIS Terra daytime Land Surface Temperatures (LST) using ground based meteorology station observations. J. Clim. 26, 1551–1560.
- Williamson, S.N., Hik, D.S., Gamon, J.A., Kavanaugh, J.L., Flowers, G.E., 2014. Estimating temperature fields from MODIS land surface temperature and air temperature observations in a sub-Arctic environment. Remote Sens. 6, 946–963.
- Zaksek, K., Schroedter-Homscheidt, M., 2009. Parameterization of air temperature in high temporal and spatial resolution from a combination of SEVIRI and MODIS instruments. ISPRS J. Photogramm. Remote Sens. 4, 414–421.